SIAM J. NUMER. ANAL.
Vol. 61, No. 2, pp. 539–561

COMPUTATIONAL LOWER BOUNDS OF THE MAXWELL EIGENVALUES*

DIETMAR GALLISTL† AND VLADISLAV OLKHOVSKIY†

Abstract. A method to compute guaranteed lower bounds to the eigenvalues of the Maxwell system in two or three space dimensions is proposed as a generalization of the method of Liu and Oishi [*SIAM J. Numer. Anal.*, 51 (2013), pp. 1634–1654] for the Laplace operator. The main tool is the computation of an explicit upper bound to the error of the Galerkin projection. The error is split into two parts. One part is controlled by a hypercircle principle and an auxiliary eigenvalue problem. The second part requires a perturbation argument for the right-hand side replaced by a suitable piecewise polynomial. The latter error is controlled through the use of the commuting quasi-interpolation by Falk and Winther and computational bounds on its stability constant. This situation is different from the Laplace operator where such a perturbation is easily controlled through local Poincaré inequalities. The practical viability of the approach is demonstrated in test cases for two and three space dimensions.

Key words. Maxwell, eigenvalues, lower bounds, quasi-interpolation, stability constants

MSC codes. 35Q61, 65N30, 65N12, 78M10

DOI. 10.1137/21M1461447

1. Introduction.

This paper is devoted to the computation of guaranteed lower bounds of the Maxwell eigenvalues. The Maxwell eigenvalue problem over a suitable bounded domain Ω in dimension $d=2$ or $d=3$ seeks eigenpairs (λ, u) with nontrivial u such that

$$(-1)^{d-1}\,\mathrm{Curl}\,\mathrm{rot}\,u = \lambda u \text{ in } \Omega \quad \text{and} \quad u \wedge \nu = 0 \text{ on } \partial\Omega. \tag{1.1}$$

Here, ν is the outer unit normal to $\partial\Omega$ and $u\wedge\nu$ is the tangential trace of u. The usual rotation (or curl) operator is denoted by rot, while its formal adjoint is denoted by Curl; precise definitions are given below. The rot operator has an infinite-dimensional kernel containing all admissible gradient fields, leading to an eigenvalue $\lambda = 0$ of infinite multiplicity. Sorting out this eigenvalue in numerical computations requires the incorporation of a divergence-free constraint. In the setting of rot-conforming finite elements, the divergence constraint is necessarily imposed in a discrete weak form because simultaneous rot- and div-conformity may lead to nondense and thus wrong approximations [14, 32]. In conclusion, a variational form of (1.1) in an energy space V is in general approximated with a nonconforming discrete space $V_h \not\subseteq V$ and no monotonicity principles are applicable for a comparison of discrete and true eigenvalues. Upper eigenvalue bounds can be expected from discontinuous Galerkin schemes [9], but the practically more interesting question of guaranteed lower bounds has remained open until the contributions [4, 5]. For a detailed exposition of the eigenvalue problem and its numerical approximation, the reader is referred to [27, 32, 6] and the references therein.

*Received by the editors November 23, 2021; accepted for publication (in revised form) November 15, 2022; published electronically March 13, 2023.
https://doi.org/10.1137/21M1461447
Funding: The work of the first author was supported by the European Research Council ERC Starting Grant DAFNE, grant 891734.

†Friedrich-Schiller-Universität Jena, Institut für Mathematik, 07743 Jena, Germany (dietmar.gallistl@uni-jena.de, vladislav.olkhovskiy@uni-jena.de).

© 2023 Dietmar Gallistl And Vladislav Olkhovskiy

In the finite element framework for coercive operators in some Hilbert space V (e.g., the Laplacian), guaranteed lower eigenvalue bounds were successfully derived by the independent contributions [31] and [11], which basically follow the same reasoning, illustrated here for the first eigenpair (λ, u) of a variational eigenvalue problem,

$$a(u,v) = \lambda b(u,v) \quad \text{for all } v \in V$$

with inner products a and b and corresponding norms $\|\cdot\|_a$ and $\|\cdot\|_b$. For a (possibly nonconforming) discretization V_h with the first discrete eigenpair (λ_h, u_h), the discrete Rayleigh–Ritz principle [38] implies

$$\lambda_h \|v_h\|_b^2 \leq \|v_h\|_a^2$$

for any $v_h \in V_h$. Given an a-orthogonal projection operator G_h (assuming a is defined on the sum $V + V_h$), this and some elementary algebraic manipulations show

$$\lambda_h \|G_h u\|_b^2 \leq \|G_h u\|_a^2 \leq \|u\|_a^2 - \|u - G_h u\|_a^2.$$

Assuming the normalization $\|u\|_b = 1$ so that $\|u\|_a^2 = \lambda$, it turns out that explicit control of $\|u - G_h u\|_b$ by $\|u - G_h u\|_a$ yields a computational lower bound. In [31] G_h is the standard Galerkin projection, while in [11] it is the interpolation operator in a Crouzeix–Raviart method. Further approaches to the computation of lower eigenvalue bounds were provided by [37, 10].

In this paper we aim at extending the idea of [31] to the Maxwell eigenvalue problem (1.1) discretized with lowest-order Nédélec (edge) elements [32]. The main novelty in contrast to [31] is the guaranteed computational control of the Galerkin error in a linear Maxwell system with right-hand-side f. In general, the estimate takes the format

$$\|u - u_h\|_a \leq M_h \|f\|_b$$

with a mesh-dependent number M_h, for which we propose a computational upper bound in this paper. In [31] such a bound is achieved for the Laplacian by splitting f in a piecewise polynomial part f_h and some remainder. The first part of the error is quantified through a hypercircle principle [8] and an auxiliary global eigenvalue problem. This idea goes back to the work [28] on a posteriori error estimators and was used in the context of eigenvalue problems by [31, 34, 29, 30]. The second part of the error is—in the case of the Laplacian, where f_h is simply the piecewise mean of f—easily controlled because it reduces to elementwise Poincaré inequalities whose constants can be explicitly bounded [33]. In the present case of the Maxwell system, the situation is more involved. The rot operator maps the Nédélec space to the divergence-free Raviart–Thomas elements [7], and the L^2-orthogonal projection to the latter is nonlocal and explicit bounds on that projection are unknown. In order to obtain a computable bound, we make use of recent developments of finite element exterior calculus [3, 2], namely the Falk–Winther projection [18]. This family of operators commutes with the exterior derivative and is locally defined, so that it is actually computable. Practical implementations of the operator have been used in the context of numerical homogenization [22, 25, 26]. In this work, the advantage of the local construction is that the involved stability constant can be computationally bounded from above. In a perturbation argument for the Maxwell system, this tool replaces the Poincaré inequality from the Laplacian case. The bounds are achieved by solving local discrete eigenvalue problems combined with standard estimates.

The main result is a computabe upper bound $\hat{M}_h$ to M_h, which results in the guaranteed lower bound

$$\frac{\lambda_h}{1+\hat{M}_h^2\lambda_h} \leq \lambda$$

from Theorem 4.1 for the kth Maxwell eigenvalue λ. The quantities on the left-hand side are the kth discrete eigenvalue λ_h and the computable mesh-dependent number $\hat{M}_h$. In particular, the computation of $\hat{M}_h$ involves guaranteed control over the bound for the Galerkin error in a linear Maxwell problem and the local stability constants of the Falk–Winther interpolation. The guaranteed computational bound $\hat{M}_h$ for M_h is carefully described in this paper. The mesh-dependent quantity M_h is required to be uniform with respect to the right-hand-side f and is therefore related to elliptic regularity of the linear Maxwell problem on the specific domain of interest. On polytopal domains it is expected to scale like the power h^s of the maximum mesh size h with some exponent $0 < s \leq 1$. This limits efficient computations to the case of lowest-order Nédélec (edge) elements. Such limitation is also encountered in the existing works [11, 31, 29] for the Laplacian.

The remaining parts of this article are organized as follows. Section 2 lists preliminaries on the Maxwell problem, discrete spaces, and the Falk–Winther interpolation. Guaranteed computational bounds on the Galerkin error are presented in section 3. The lower eigenvalue bounds are shown in section 4, the practical computation of the relevant constants is described in section 5, and actual computations are shown in the numerical experiments of section 6. The remarks of section 7 conclude this paper.

2. Preliminaries.

2.1. Notation. Let $\Omega \subseteq \mathbb{R}^d$ for $d \in \{2,3\}$ be a bounded and open polytopal Lipschitz domain, which we assume to be contractible. The involved differential operators read

$$\operatorname{rot} v = \partial_1 v_2 - \partial_2 v_1 \text{ for } d=2 \quad \text{and} \quad \operatorname{rot} v = \begin{pmatrix} \partial_2 v_3 - \partial_3 v_2 \\ \partial_3 v_1 - \partial_1 v_3 \\ \partial_1 v_2 - \partial_2 v_1 \end{pmatrix} \text{ for } d=3.$$

For the formal adjoint operators we write

$$\operatorname{Curl} \phi = \begin{pmatrix} -\partial_2 \phi \\ \partial_1 \phi \end{pmatrix} \text{ for } d=2 \quad \text{and} \quad \operatorname{Curl} = \operatorname{rot} \text{ for } d=3$$

(ϕ is a scalar function for $d=2$) so that the integration-by-parts formula

$$\int_\Omega \phi \operatorname{rot} v\, dx = (-1)^{d-1} \int_\Omega \operatorname{Curl} \phi \cdot v\, dx$$

holds for sufficiently regular scalar functions ($d=2$) or vector fields ($d=3$) ϕ and vector fields v with vanishing tangential trace over $\partial\Omega$.

Standard notation on Lebesgue and Sobolev spaces is employed throughout this paper. Given any open set $\omega \subseteq \mathbb{R}^d$, the $L^2(\omega)$ inner product is denoted by $(\cdot,\cdot)_{L^2(\omega)}$ with the norm $\|\cdot\|_{L^2(\omega)}$. The usual L^2-based first-order Sobolev space is denoted by $H^1(\Omega)$ and $H^1_0(\Omega)$ is the subspace with vanishing trace over $\partial\Omega$. The space of L^2 vector fields over Ω with weak divergence in $L^2(\Omega)$ is denoted by $H(\operatorname{div},\Omega)$, and the subspace of divergence-free vector fields reads $H(\operatorname{div}^0,\Omega)$. The space of $L^2(\Omega)$ vector fields with weak rotation in $L^2(\Omega)$ is denoted by $H(\mathrm{rot},\Omega)$, while its subspace with vanishing tangential trace is denoted by $H_0(\mathrm{rot},\Omega)$.

In the context of eigenvalue problems, the L^2 inner product is also denoted by $b(\cdot,\cdot)$ and the L^2 norm is denoted by $\|\cdot\|_b$.

On $H_0(\mathrm{rot},\Omega)$, we define the bilinear form

$$a(v,w) := (\mathrm{rot}\, v, \mathrm{rot}\, w)_{L^2(\Omega)} \quad \text{for any } v,w \in H_0(\mathrm{rot},\Omega).$$

Let $V := H_0(\mathrm{rot},\Omega) \cap H(\mathrm{div}^0,\Omega)$. On V, the form a is an inner product [32, Corollary 4.8] and the seminorm $\|\cdot\|_a = \sqrt{a(\cdot,\cdot)}$ is a norm on V. Given a divergence-free right-hand-side $f \in H(\mathrm{div}^0,\Omega)$, the linear Maxwell problem seeks $u \in V$ such that

$$a(u,v) = b(f,v) \quad \text{for all } v \in V. \tag{2.1}$$

It is well known [32] and needed in some arguments of this article that (2.1) is even satisfied for all test functions v from the larger space $H_0(\mathrm{rot},\Omega)$.

Let $\mathcal{T}$ be a regular simplicial triangulation of Ω. The diameter of any $T \in \mathcal{T}$ is denoted by h_T and $h_{\max} := \max_{T\in\mathcal{T}} h_T$ is the maximum mesh size. Given any $T \in \mathcal{T}$, the space of first-order polynomial functions over T is denoted by $P_1(T)$. The lowest-order standard finite element space (with or without homogeneous Dirichlet boundary conditions) is denoted by

$$S^1(\mathcal{T}) := \{v \in H^1(\Omega) : \forall T \in \mathcal{T}, v|_T \in P_1(T)\} \text{ and } S^1_0(\mathcal{T}) := H^1_0(\Omega) \cap S^1(\mathcal{T}).$$

The space of lowest-order edge elements [32, 7] reads

$$\begin{aligned}\mathcal{N}_0(\mathcal{T}) = \{v \in H(\mathrm{rot},\Omega) : \forall T \in \mathcal{T}\ \exists \alpha_T \in \mathbb{R}^d\ \exists \beta_T \in P_1(T)^d \forall x \in T :\\ v(x) = \alpha_T + \beta_T(x) \text{ and } \beta_T(x)\cdot x = 0\}\end{aligned}$$

and we denote

$$\mathcal{N}_{0,D}(\mathcal{T}) := \mathcal{N}_0(\mathcal{T}) \cap H_0(\mathrm{rot},\Omega).$$

The approximation of (2.1) with edge elements uses the space

$$V_h = \{\psi_h \in \mathcal{N}_{0,D}(\mathcal{T}) : \forall v_h \in S^1_0(\mathcal{T})\ (\nabla v_h, \psi_h)_{L^2(\Omega)} = 0\}. \tag{2.2}$$

The elements of V_h are weakly divergence-free and in general need not be elements of V, i.e., $V_h \not\subseteq V$. It is known [32] that a is an inner product on V_h. The finite element system seeks $u_h \in V_h$ such that

$$a(u_h, v_h) = b(f, v_h) \quad \text{for all } v_h \in V_h. \tag{2.3}$$

We remark that, in practical computations, systems like (2.3) are solved as mixed systems with a Lagrange multiplier enforcing the linear constraint in (2.2). Given u, its approximation $u_h = G_h u$ is called the Galerkin projection. This terminology is justified by the fact that the approach is conforming when viewed in a saddle-point setting. In particluar, since (2.1) is satisfied for all $v \in H_0(\mathrm{rot},\Omega)$, the following “Galerkin orthogonality” is valid:

$$a(u - u_h, v_h) = 0 \quad \text{for all } v_h \in V_h. \tag{2.4}$$

The Raviart–Thomas finite element space [7] is defined as

$$\begin{aligned}RT_0(\mathcal{T}) := \{v \in H(\mathrm{div},\Omega) : \forall T \in \mathcal{T} \exists (\alpha_T, \beta_T) \in \mathbb{R}^d \times \mathbb{R}\\ \forall x \in T, v|_T(x) = \alpha_T + \beta_T x\}.\end{aligned}$$

$$\begin{tikzcd}
H(\mathrm{Curl},\Omega) \arrow[r, "\mathrm{Curl}"] \arrow[d, "\pi^{\mathrm{Curl}}"] & H(\mathrm{div},\Omega) \arrow[d, "\pi^{\mathrm{div}}"] \\
\mathcal{S}_h \arrow[r, "\mathrm{Curl}"] & RT_0(\mathcal{T})
\end{tikzcd}$$

FIG. 1. *Commuting diagram of the Falk–Winther operator.*

2.2. Falk–Winther interpolation. Given a regular triangulation $\mathcal{T}$ and any element $T \in \mathcal{T}$, the element patch built by the simplices having nontrivial intersection with T is defined as

$$\omega_T := \mathrm{int}(\cup\{K \in \mathcal{T} : K \cap T \neq \emptyset\}).$$

There is a projection $\pi^{\mathrm{div}} : H(\mathrm{div},\Omega) \to RT_0(\mathcal{T})$ with local stability in the sense that there exist constants $C_{1,\mathrm{div}}$, $C_{2,\mathrm{div}}$ such that for any $T \in \mathcal{T}$ and any $v \in H(\mathrm{div},\Omega)$ we have

$$\|\pi^{\mathrm{div}} v\|_{L^2(T)} \leq C_{1,\mathrm{div}} \|v\|_{L^2(\omega_T)} + h_T C_{2,\mathrm{div}} \|\mathrm{div}\ v\|_{L^2(\omega_T)}. \tag{2.5}$$

Furthermore, there is a projection $\pi^{\mathrm{Curl}} : H(\mathrm{Curl},\Omega) \to \mathcal{S}_h$ where

$$H(\mathrm{Curl},\Omega) = \begin{cases} H^1(\Omega;\mathbb{R}^2) & \text{if } d = 2 \\ H(\mathrm{rot},\Omega) & \text{if } d = 3 \end{cases} \quad \text{and} \quad \mathcal{S}_h = \begin{cases} S^1(\mathcal{T}) & \text{if } d = 2 \\ \mathcal{N}_0(\mathcal{T}) & \text{if } d = 3 \end{cases}$$

with constants $C_{1,\mathrm{Curl}}$, $C_{2,\mathrm{Curl}}$ such that for any $T \in \mathcal{T}$ and any $v \in H(\mathrm{Curl},\Omega)$ we have

$$\|\pi^{\mathrm{Curl}} v\|_{L^2(T)} \leq C_{1,\mathrm{Curl}} \|v\|_{L^2(\omega_T)} + h_T C_{2,\mathrm{Curl}} \|\mathrm{Curl}\ v\|_{L^2(\omega_T)}. \tag{2.6}$$

The crucial property is that these two operators commute with the exterior derivative in the sense that $\pi^{\mathrm{div}}\,\mathrm{Curl} = \mathrm{Curl}\,\pi^{\mathrm{Curl}}$. The corresponding commuting diagram is displayed in Figure 1. For the construction of the operators π^{div} and π^{Curl}, the reader is referred to [18] and section 5.3 below.

3. Bounds on the Galerkin projection. The goal of this section is a fully computable bound on the Galerkin error.

3.1. L^2 error control. From elliptic regularity theory (see [32, Theorem 3.50] and [15]), it is known that the solution $u \in V$ to (2.1) satisfies

$$\|u\|_{H^s(\Omega)} + \|\mathrm{rot}\, u\|_{H^s(\Omega)} \leq C\|f\|_b$$

for some positive $s > 1/2$, where $\|\cdot\|_{H^s(\Omega)}$ is the usual fractional-order Sobolev space [32]. The Galerkin property (2.4) and well-known interpolation error estimates [32, Theorem 5.25] show that

$$\|u - G_h u\|_a \leq \inf_{v_h \in V_h} \|u - v_h\|_a \leq C h^s \|\mathrm{rot}\, u\|_{H^s(\Omega)}. \tag{3.1}$$

Hence, there exists a mesh-dependent (but f-independent) number M_h such that

$$\|u - G_h u\|_a \le M_h \|f\|_b, \tag{3.2}$$

where it is understood that M_h is the optimal choice (uniformly in $\|f\|_b$). On convex domains, M_h is proportional to the mesh size h, while in general, reduced regularity implies that M_h is proportional to h^s with some $0 < s \le 1$. Theorem 3.6 below states a computable upper bound $M_h \le \hat{M}_h$.

Given some $u \in V$, the Galerkin approximation $G_h u$ is usually not divergence-free and therefore possesses a nontrivial L^2 orthogonal decomposition

$$G_h u = \nabla\phi + R \tag{3.3}$$

with $\phi \in H_0^1(\Omega)$ and $R \in H(\mathrm{div}^0, \Omega)$. The inclusion $G_h u \in H_0(\mathrm{rot}, \Omega)$ furthermore shows that $R \in V$. The following lemma states an L^2 error estimate. The proof uses the classical Aubin–Nitsche duality technique.

LEMMA 3.1. *The divergence-free part $u - R$ of the error $u - G_h u$ satisfies the following error estimate:*

$$\|u - R\|_b \le M_h \|u - G_h u\|_a.$$

Proof. The error $e := u - R$ is divergence-free and thus $e \in V$. There exists a unique solution $z \in V$ satisfying

$$a(z, v) = b(e, v) \quad \text{for all } v \in V.$$

Since $e \in V$, we infer with the symmetry of a and $\mathrm{rot}\,\nabla = 0$ that

$$\|e\|_b^2 = b(e, e) = a(z, e) = a(e, z) = a(u - G_h u, z).$$

The Galerkin property (2.4) shows that $u - G_h u$ is a-orthogonal to any element of V_h. Thus

$$\|e\|_b^2 = a(u - G_h u, z - G_h z) \le \|u - G_h u\|_a \, \|z - G_h z\|_a.$$

The application of (3.2) to z with right-hand-side e reveals that the Galerkin error $\|z - G_h z\|_a$ is bounded by $M_h \|e\|_b$, which implies the asserted bound. ∎

3.2. Perturbation of the right-hand side. In this section, we quantify the error that arises in the solution of the linear Maxwell system when the right-hand-side f is replaced by a piecewise polynomial approximation f_h.

The regular decomposition [17, Proposition 4.1] states that there exists a constant C_{RD} such for that every $f \in H(\mathrm{div}^0, \Omega)$ there exists $\beta \in H^1(\Omega; \mathbb{R}^{2d-3})$ such that

$$\mathrm{Curl}\,\beta = f \qquad \text{and} \qquad \|D\beta\|_{L^2(\Omega)} \le C_{RD} \|f\|_{L^2(\Omega)}, \tag{3.4}$$

where $D\beta$ denotes the derivative (Jacobian matrix) of the vector field β. We remark that in the two-dimensional case the field $\mathrm{Curl}\,\beta$ is a rotation of $D\beta$ so that $C_{RD} = 1$ if $d = 2$.

Given $T \in \mathcal{T}$ and its element patch ω_T, the Poincaré inequality states for any H^1 function v with vanishing average over ω_T that $\|v\|_{L^2(\omega_T)} \le C(T)\|Dv\|_{L^2(\omega_T)}$ with a constant $C(T)$ proportional to h_T. By $\tilde{c}$ we denote the smallest constant such that

$$\|v\|_{L^2(\omega_T)} \le h_T \tilde{c} \|Dv\|_{L^2(\omega_T)}$$

holds for all such functions uniformly in $T \in \mathcal{T}$.

Recall that, due to its commutation property, the Falk–Winther interpolation π^{div} maps $H(\mathrm{div}^0,\Omega)$ to $RT_0(\mathcal{T})\cap H(\mathrm{div}^0,\Omega)$. We denote the overlap constant of element patches by

$$C_{OL} = \max_{T\in\mathcal{T}} \operatorname{card}\{K\in\mathcal{T} : T\subseteq \overline{\omega_K}\}.$$

LEMMA 3.2. *Let $f\in H(\mathrm{div}^0,\Omega)$ and let $\tilde f = \pi^{\mathrm{div}} f \in RT_0(\mathcal{T})\cap H(\mathrm{div}^0,\Omega)$ be its Falk–Winther interpolation. Let u and $\tilde u$ denote the solution to* (2.1) *with right-hand-side f and $\tilde f$, respectively. Then*

$$\|u-\tilde u\|_a \le \sqrt{C_{OL}}\, h_{\max}\hat C \|f\|_{L^2(\Omega)}$$

for the constant

$$\hat C := \begin{cases} (1+C_{1,\mathrm{Curl}})\tilde c + C_{2,\mathrm{Curl}} & \text{if } d=2,\\ \sqrt{2(((1+C_{1,\mathrm{Curl}})\tilde c C_{RD})^2 + C_{2,\mathrm{Curl}}^2)} & \text{if } d=3.\end{cases}$$

Proof. Abbreviate $e := u-\tilde u$. The solution properties imply

$$\|u-\tilde u\|_a^2 = a(u-\tilde u, e) = b(f-\tilde f, e) = b(f-\pi^{\mathrm{div}} f, e).$$

From the regular decomposition (3.4) and the commuting property of the operators π^{div}, π^{Curl} we obtain

$$f - \pi^{\mathrm{div}} f = \operatorname{Curl}\beta - \pi^{\mathrm{div}}\operatorname{Curl}\beta = \operatorname{Curl}(\beta - \pi^{\mathrm{Curl}}\beta).$$

Thus, integration by parts and the homogeneous boundary conditions of e imply

$$\begin{aligned} b(f-\pi^{\mathrm{div}} f, e) &= b(\operatorname{Curl}(\beta-\pi^{\mathrm{Curl}}\beta), e)\\ &= (-1)^{d-1} b(\beta - \pi^{\mathrm{Curl}}\beta, \operatorname{rot} e) \le \|\beta-\pi^{\mathrm{Curl}}\beta\|_b \|e\|_a. \end{aligned}$$

The combination with the above chain of identities implies

$$\|u-\tilde u\|_a \le \|\beta - \pi^{\mathrm{Curl}}\beta\|_b. \tag{3.5}$$

Let $T\in\mathcal{T}$ be arbitrary. Since π^{Curl} locally preserves constants, we obtain for the patch average

$$\bar\beta := ⨍_{\omega_T} \beta\, dx$$

that the difference $\beta - \pi^{\mathrm{Curl}}\beta$ can be split with the triangle inequality and the inclusion $T\subseteq\overline{\omega_T}$ as follows:

$$\|\beta-\pi^{\mathrm{Curl}}\beta\|_{L^2(T)} \le \|\beta-\bar\beta\|_{L^2(\omega_T)} + \|\pi^{\mathrm{Curl}}(\beta-\bar\beta)\|_{L^2(T)}.$$

Estimate (2.6) with $\operatorname{Curl}\beta = f$ followed by the Poincaré inequality on ω_T with constant $h_T\tilde c$ thus reveal

$$\|\beta-\pi^{\mathrm{Curl}}\beta\|_{L^2(T)} \le h_T\tilde c(1+C_{1,\mathrm{Curl}})\|D\beta\|_{L^2(\omega_T)} + C_{2,\mathrm{Curl}} h_T \|f\|_{L^2(\omega_T)}.$$

This local result generalizes to the whole domain Ω as follows:

$$\begin{aligned}\|\beta-\pi^{\mathrm{Curl}}\beta\|_b^2 &= \sum_{T\in\mathcal{T}} \|\beta-\pi^{\mathrm{Curl}}\beta\|_{L^2(T)}^2 \\ &\le \sum_{T\in\mathcal{T}} (h_T\tilde{c}(1+C_{1,\mathrm{Curl}})\|D\beta\|_{L^2(\omega_T)} + C_{2,\mathrm{Curl}}h_T\|f\|_{L^2(\omega_T)})^2. \end{aligned} \tag{3.6}$$

If $d=2$ we have the identity $\|D\beta\|_{L^2(\omega_T)} = \|f\|_{L^2(\omega_T)}$ and therefore conclude

$$\begin{aligned}\|\beta-\pi^{\mathrm{Curl}}\beta\|_b^2 &\le \sum_{T\in\mathcal{T}} h_T^2(\tilde{c}(1+C_{1,\mathrm{Curl}})+C_{2,\mathrm{Curl}})^2\|f\|_{L^2(\omega_T)}^2 \\ &\le C_{OL}h_{\max}^2(\tilde{c}(1+C_{1,\mathrm{Curl}})+C_{2,\mathrm{Curl}})^2\|f\|_{L^2(\Omega)}^2.\end{aligned}$$

The squared expression in parentheses on the right-hand side equals $\hat{C}$ if $d=2$, whence the assertion follows in that case. If $d=3$, we again use (3.6) and compute

$$\begin{aligned}\|\beta-\pi^{\mathrm{Curl}}\beta\|_b^2 &\le 2\sum_{T\in\mathcal{T}} h_T^2\left((\tilde{c}(1+C_{1,\mathrm{Curl}})\|D\beta\|_{L^2(\omega_T)})^2 + (C_{2,\mathrm{Curl}}\|f\|_{L^2(\omega_T)})^2\right) \\ &\le 2C_{OL}h_{\max}^2\left((\tilde{c}(1+C_{1,\mathrm{Curl}})\|D\beta\|_{L^2(\Omega)})^2 + (C_{2,\mathrm{Curl}}\|f\|_{L^2(\Omega)})^2\right).\end{aligned}$$

We estimate $\|D\beta\|_{L^2(\Omega)}$ with (3.4) and obtain

$$\|\beta-\pi^{\mathrm{Curl}}\beta\|_b \le \sqrt{2C_{OL}}h_{\max}\hat{C}\|f\|_{L^2(\Omega)}.$$

The combination with (3.5) concludes the proof. ∎

3.3. Error bound on the Galerkin projection. We denote the space of divergence-free Raviart–Thomas functions by $X_h := RT_0(\mathcal{T})\cap H(\mathrm{div}^0,\Omega)$. Given $f_h\in X_h$, let

$$\mathcal{S}_{f_h} := \{v_h\in\mathcal{S}_h : \mathrm{Curl}\, v_h = (-1)^{d-1}f_h\}.$$

Define

$$\kappa_h := \max_{f_h\in X_h\setminus\{0\}} \min_{v_h\in V_h} \min_{\tau_h\in\mathcal{S}_{f_h}} \frac{\|\tau_h - \mathrm{rot}\, v_h\|_{L^2(\Omega)}}{\|f_h\|_{L^2(\Omega)}}. \tag{3.7}$$

The next lemma states that, for discrete data, the Galerkin error can be quantified through κ_h.

LEMMA 3.3. *Let $f_h\in X_h$, and let $\tilde{u}\in V$ and $\tilde{u}_h\in V_h$ be solutions to* (2.1) *and* (2.3)*, respectively, with right-hand-side $f=f_h$. Then the following computable error estimate holds:*

$$\|\tilde{u}-\tilde{u}_h\|_a \le \kappa_h\|f_h\|_b.$$

Proof. Let $v_h\in V_h$ be arbitrary and let $\tau_h\in\mathcal{S}_{f_h}$. Integration by parts implies the orthogonality

$$(\tau_h - \mathrm{rot}\,\tilde{u}, \mathrm{rot}(\tilde{u}-v_h))_{L^2(\Omega)} = 0.$$

Thus the following hypercircle identity holds:

$$\|\tau_h - \mathrm{rot}\,\tilde{u}\|_{L^2(\Omega)}^2 + \|\mathrm{rot}(\tilde{u}-v_h)\|_{L^2(\Omega)}^2 = \|\tau_h - \mathrm{rot}\, v_h\|_{L^2(\Omega)}^2. \tag{3.8}$$

Thus,

$$\|\tilde u - v_h\|_a = \|\operatorname{rot}(\tilde u - v_h)\|_{L^2(\Omega)} \le \min_{\tau \in \mathcal{S}_{f_h}} \|\tau_h - \operatorname{rot} v_h\|_{L^2(\Omega)}.$$

The left-hand side is minimal for $\tilde u_h$ among all elements $v_h \in V_h$, whence

$$\|\tilde u - \tilde u_h\|_a \le \min_{v_h \in V_h} \min_{\tau \in \mathcal{S}_{f_h}} \|\tau_h - \operatorname{rot} v_h\|_{L^2(\Omega)} \le \kappa_h \|f_h\|_{L^2(\Omega)},$$

where the last estimate follows from the definition (3.7). ∎

Remark 3.4. Hypercircle (or Prager–Synge) identities like (3.8) are often used in the context of a posteriori error estimation [8, 35, 36, 13].

Remark 3.5. The asymptotic convergence rate of κ_h is that of the sum of the primal and dual mixed finite element error. This can be seen from taking the minimum over v_h and τ_h in the hypercircle relation (3.8) for the "worst" L^2-normalized right-hand-side f_h. Thus, κ_h is proportional to h^s with the elliptic regularity index s from (3.1).

For possibly nondiscrete f, the Galerkin error is bounded by the following perturbation argument.

THEOREM 3.6. *Given $f \in H(\operatorname{div}^0, \Omega)$, let $u \in V$ solve* (2.1) *and let $u_h \in V_h$ solve* (2.3)*. Let $\hat M_h$ with*

$$\hat M_h \ge (h_{\max} \hat C + \kappa_h C_{1,\operatorname{div}}) \sqrt{C_{OL}}$$

(with $\hat C$ from Lemma 3.2*) be given. Then, the following error bound is satisfied:*

$$\|u - u_h\|_a \le \hat M_h \|f\|_{L^2(\Omega)}.$$

In particular, $M_h \le \hat M_h$.

Proof. Let $f_h = \pi^{\operatorname{div}} f$ denote the Falk–Winther interpolation of f and denote as in Lemma 3.3 by $\tilde u$ and $\tilde u_h$ the solutions with respect to f_h. Since $u_h \in V_h$ minimizes the error $\|u - v_h\|_a$ among all $v_h \in V_h$, we have $\|u - u_h\|_a \le \|u - \tilde u_h\|_a$. The triangle inequality then leads to

$$\|u - u_h\|_a \le \|u - \tilde u\|_a + \|\tilde u - \tilde u_h\|_a. \tag{3.9}$$

The second term on the right-hand side is bounded through Lemma 3.3 as follows:

$$\|\tilde u - \tilde u_h\|_a \le \kappa_h \|f_h\|_{L^2(\Omega)} = \kappa_h \|\pi^{\operatorname{div}} f\|_{L^2(\Omega)}.$$

The local stability (2.5) of π^{div} (note that $\operatorname{div} f = 0$) and the overlap of element patches imply

$$\|\pi^{\operatorname{div}} f\|^2_{L^2(\Omega)} = \sum_{T \in \mathcal{T}} \|\pi^{\operatorname{div}} f\|^2_{L^2(T)} \le \sum_{T \in \mathcal{T}} C^2_{1,\operatorname{div}} \|f\|^2_{L^2(\omega_T)} \le C_{OL} C^2_{1,\operatorname{div}} \|f\|^2_{L^2(\Omega)}.$$

Thus,

$$\|\tilde u - \tilde u_h\|_a \le \kappa_h \sqrt{C_{OL}} C_{1,\operatorname{div}} \|f\|_{L^2(\Omega)}. \tag{3.10}$$

The first term on the right-hand side of (3.9) is bounded through Lemma 3.2 by $\sqrt{C_{OL}}h_{\max}\hat{C}$. The combination of this bound with (3.9) and (3.10) concludes the proof. ∎

The foregoing theorem shows that a computable upper bound $\hat{M}_h$ to M_h can be found if values or upper bounds of $\hat{C}$, κ_h, $C_{1,\mathrm{div}}$ are available. Their computation is described in section 5.

4. Eigenvalue problem and lower bound. The Maxwell eigenvalue problem seeks pairs $(\lambda, u) \in \mathbb{R} \times V$ with $\|u\|_b = 1$ such that

$$a(u, v) = \lambda b(u, v) \quad \text{for all } v \in V. \tag{4.1}$$

The condition $u \in V$ implies that $\operatorname{div} u = 0$ and, thus, the noncompact part of the spectrum of the Curl rot operator (corresponding to gradient fields as eigenfunctions) is sorted out in this formulation. It is well known [32] that the eigenvalues to (4.1) form an infinite discrete set

$$0 < \lambda_1 \le \lambda_2 \le \dots \quad \text{with } \lim_{j\to\infty} \lambda_j = \infty.$$

The discrete counterpart seeks $(\lambda_h, u_h) \in \mathbb{R} \times V_h$ with $\|u_h\|_b = 1$ such that

$$a(u_h, v_h) = \lambda_h b(u_h, v_h) \quad \text{for all } v_h \in V_h. \tag{4.2}$$

We now focus on the kth eigenpair (λ, u) and its approximation (λ_h, u_h). Recall M_h from (3.2), which in practice is bounded by $\hat{M}_h$ from Theorem 3.6.

THEOREM 4.1. *Let* $(\lambda, u) \in \mathbb{R} \times V$ *with* $\|u\|_b = 1$ *be the* k*th eigenpair to* (4.1) *and* $(\lambda_h, u_h) \in \mathbb{R} \times V_h$ *with* $\|u_h\|_b = 1$ *be the* k*th discrete eigenpair to* (4.2). *The following lower bound holds:*

$$\frac{\lambda_h}{1 + M_h^2 \lambda_h} \le \lambda.$$

In particular, we have the computable guaranteed lower bound

$$\frac{\lambda_h}{1 + \hat{M}_h^2 \lambda_h} \le \lambda$$

with $\hat{M}_h$ *from Theorem* 3.6.

Proof. We denote an a-orthonormal set of first k eigenfunctions by $u_1, \dots u_k$. If $k = 1$, we denote the first eigenfunction by $v := u_1$ and note that the discrete Rayleigh–Ritz principle implies $\lambda_h \|G_h v\|_b^2 \le \|G_h v\|_a^2$. If $k \ge 2$, we consider in a first case that the space spanned by $G_h u_1, \dots, G_h u_k$ has dimension k. The discrete Rayleigh–Ritz principle [38] for the kth discrete eigenvalue λ_h states

$$\lambda_h = \min_{V_h^{(k)} \subseteq V_h} \max_{v_h \in V_h^{(k)} \setminus \{0\}} \frac{\|v_h\|_a^2}{\|v_h\|_b^2} \le \max_{v_h \in \operatorname{span}\{G_h u_1, \dots, G_h u_k\} \setminus \{0\}} \frac{\|v_h\|_a^2}{\|v_h\|_b^2},$$

where the minimum runs over all k-dimensional subspaces $V_h^{(k)}$ of V_h. There exist real coefficients $\xi_1, \dots, \xi_k$ with $\sum_{j=1}^k \xi_j^2 = 1$ such that the maximizer on the right-hand side equals $G_h v$ for $v = \sum_{j=1}^k \xi_j u_j$. Recall the Helmholtz decomposition (3.3) with the divergence-free part R of v. The above Rayleigh–Ritz principle implies

$$\lambda_h \leq \frac{\|G_h v\|_a^2}{\|G_h v\|_b^2}$$

and therefore (for $k \geq 1$)

$$\lambda_h \|R\|_b^2 \leq \lambda_h \|G_h v\|_b^2 \leq \|G_h v\|_a^2. \tag{4.3}$$

We expand the square on the left-hand side, use that $\|v\|_b^2 = 1$, and use the Young inequality with an arbitrary $0 < \delta < 1$ to infer

$$\|R\|_b^2 = \|R - v\|_b^2 + 1 + 2b(R - v, v) \geq (1 - \delta^{-1})\|R - v\|_b^2 + (1 - \delta)$$

(note that $1 - \delta^{-1} < 0$). The combination with Lemma 3.1 results in

$$\lambda_h \|R\|_b^2 \geq \lambda_h \left((1 - \delta^{-1}) M_h^2 \|G_h v - v\|_a^2 + (1 - \delta)\right). \tag{4.4}$$

The Galerkin orthogonality (2.4) in the a-product and the estimate $\|v\|_a^2 \leq \lambda$ for the right-hand side of (4.3) result in

$$\|G_h v\|_a^2 \leq \lambda - \|v - G_h v\|_a^2. \tag{4.5}$$

The choice $\delta = (\lambda_h M_h^2)/(1 + \lambda_h M_h^2)$ and the combination of (4.3)–(4.5) result in

$$\frac{\lambda_h}{1 + M_h^2 \lambda_h} \leq \lambda. \tag{4.6}$$

In the remaining case that the space spanned by $G_h u_1, \ldots, G_h u_k$ has dimension strictly less than k, there exists a b-normalized function v in the linear hull of the functions $u_1, \ldots, u_k$ such that $G_h v = 0$. The divergence-free part R of $G_h v$ is thus zero and Lemma 3.1 implies

$$1 = \|v\|_b^2 = \|v - R\|_b^2 \leq M_h^2 \|v - G_h v\|_a^2 = M_h^2 \|v\|_a^2.$$

Since v is taken from the linear hull of the first k eigenfunctions, the orthogonality of the latter implies $\|v\|_a^2 \leq \lambda_k$. Therefore $M_h^{-2} \leq \lambda_k$ (excluding the trivial case $M_h = 0$), which implies the bound (4.6) also in the second case. The stated computable bound follows from (4.6) $M_h \leq \hat{M}_h$ and the monotonicity of the left-hand side in the proven estimate. ∎

5. Bounds on the involved constants.

This section describes how the critical constants are computed or computationally bounded.

5.1. Computation of κ_h.

In this paragraph we briefly sketch the numerical computation of κ_h. The reasoning is similar to [31], and we illustrate the extension of their approach to the Maxwell operator. Recall from subsection 3.3 the space X_h and the set $\mathcal{S}_{f_h}$ for given $f_h \in X_h$. Let furthermore $\tilde{u} \in V$ denote the solution to the linear problem (2.1) with right-hand-side f_h. Expanding squares and integration by parts then shows for any $\tau_h \in \mathcal{S}_{f_h}$ and any $v_h \in \mathcal{N}_{0,D}(\mathcal{T})$ the hypercircle identity (3.8) because $\operatorname{Curl}(\tau_h - \operatorname{rot} \tilde{u}) = 0$. Thus, the optimization problem

$$\min_{v_h \in \mathcal{N}_{0,D}(\mathcal{T})} \min_{\tau_h \in \mathcal{S}_{f_h}} \|\tau_h - \operatorname{rot} v_h\|_{L^2(\Omega)}^2$$

is equivalent to

$$\min_{v_h \in \mathcal{N}_{0,D}(\mathcal{T})} \|\mathrm{rot}\,(\tilde{u} - v_h)\|^2_{L^2(\Omega)} + \min_{\tau_h \in \mathcal{S}_{f_h}} \|\tau_h - \mathrm{rot}\,\tilde{u}\|^2_{L^2(\Omega)}.$$

The minimizer to the first term is given by the solution to the primal problem (2.3), while the minimizer to the second term is given by σ_h as part of the solution pair $(\sigma_h, \rho_h) \in \mathcal{S}_h \times X_h$ to the following (dual) saddle-point problem:

$$\begin{aligned} (\sigma_h, \tau_h)_{L^2(\Omega)} + (-1)^d (\mathrm{Curl}\,\tau_h, \rho_h)_{L^2(\Omega)} &= 0 && \text{for all } \tau_h \in \mathcal{S}_h, \\ (-1)^d (\mathrm{Curl}\,\sigma_h, \phi_h)_{L^2(\Omega)} &= -(f_h, \phi_h)_{L^2(\Omega)} && \text{for all } \phi_h \in X_h. \end{aligned}$$

This can be shown with arguments analogous to [8, Chapter 3, section 9, Lemma 9.1].

Let $T_h : X_h \to \mathcal{N}_{0,D}(\mathcal{T})$ denote the solution operator to the primal problem and let $S_h : X_h \to \mathcal{S}_h$, $R_h : X_h \to X_h$ denote the components of the solution operator to the dual problem. The operators T_h and R_h are symmetric, and straightforward calculations involving the definitions of S_h, T_h, R_h prove that the error can be represented as

$$\|\mathrm{rot}\,u_h - \sigma_h\|^2_{L^2(\Omega)} = -(f_h, T_h f_h)_{L^2(\Omega)} + (f_h, R_h f_h)_{L^2(\Omega)}.$$

The divergence-free constraint in the primal problem is practically implemented in a saddle-point fashion. In what follows, we identity the piecewise constant function f_h with its vector representation. The matrix structure of the discrete problem is as follows:

$$L \begin{pmatrix} w_1 \\ w_2 \end{pmatrix} = \begin{pmatrix} Bf_h \\ 0 \end{pmatrix}, \qquad \text{where } L := \begin{pmatrix} D & F^T \\ F & 0 \end{pmatrix}.$$

The solution can be expressed by

$$w_1 = L^{-1}(*,*)Bf_h = HBf_h,$$

where $H := L^{-1}(*,*)$ denotes the relevant rows and columns of L^{-1} for the computation of the first component of the solution.

The dual system can be implemented by introducing Lagrange multipliers related to the interior hyper-faces to enforce normal continuity. In terms of matrices, the dual system reads

$$K \begin{pmatrix} z_1 \\ z_2 \\ z_3 \end{pmatrix} = \begin{pmatrix} 0 \\ Mf_h \\ 0 \end{pmatrix}, \qquad \text{where } K := \begin{pmatrix} A & -G^T & 0 \\ G & 0 & C \\ 0 & C^T & 0 \end{pmatrix}.$$

The solution can be expressed by

$$z_2 = K^{-1}(**,**)Mf_h = \tilde{H}Mf_h,$$

where $\tilde{H} := K^{-1}(**,**)$ denotes the relevant rows and columns of K^{-1} for the computation of the second component of the solution.

Thus,

$$\|\mathrm{rot}\,u_h - \sigma_h\|^2_{L^2(\Omega)} = f_h^T B^T HBf_h + f_h^T M^T \tilde{H} M f_h = f_h^T Q f_h,$$

where $Q := B^T H B + M^T \tilde{H} M$. Then κ_h has the following representation:

$$\kappa_h = \max_{f_h \in X_h \setminus \{0\}} \frac{\|\operatorname{rot} u_h - \sigma_h\|_{L^2(\Omega)}}{\|f_h\|_{L^2(\Omega)}} = \max_{y \in \mathbb{R}^m \setminus \{0\}, C^T y = 0} \left(\frac{y^T Q y}{y^T M y} \right)^{-1/2}.$$

The constraint $C^T y = 0$ accounts for the fact that the elements of X_h are the piecewise constant vector fields satisfying normal continuity across the element boundaries. Since Q is symmetric, κ_h is the square root of the maximum eigenvalue μ of the eigenvalue problem

$$\begin{pmatrix} Q & C^T \\ C & 0 \end{pmatrix} y = \mu \begin{pmatrix} M & 0 \\ 0 & 0 \end{pmatrix} y.$$

The eigenvalue problem can be numerically solved with a power method and an inner iteration. The idea of this method is similar to the Lanczos method with an inner iteration [23].

5.2. Bound on local Poincaré constants. It is well known that the Poincaré constant over a domain ω equals $\mu^{-1/2}$ for the first Laplace–Neumann eigenvalue μ. We compute upper bounds on the Poincaré constant of element patches by determining lower bounds on the first Neumann eigenvalue. To this end, we use the method of [11] (with improved constants from [12]) on a subtriangulation of the patch. In our computation, for every possible cell patch ω_T a Neumann eigenvalue problem for the Laplacian is solved. The lower bound for the first eigenvalue λ_1 is given by $\hat{\lambda}_1$

$$\hat{\lambda}_1 := \frac{\lambda_{CR,1}}{1 + \kappa^2 \lambda_{CR,1} H^2} \leq \lambda_1,$$

where $\kappa^2 \approx 0.0889$ in two dimensions and $\kappa^2 \approx 1.0083$ in three dimensions, H is the maximum mesh size of the subtriangulation of ω_T, and $\lambda_{CR,1}$ is the first discrete eigenvalue computed by the Crouzeix–Raviart method. We remark that improved values for κ were worked out in [29]. To get an adequate lower bound of the Poincaré constant we use a submesh generated by three uniform refinements of the patch. We divide the resulting Poincaré constant $\operatorname{diam}(\omega_T)\tilde{c}$ by $\operatorname{diam}(\omega_T)$ and obtain a mesh-size independent upper bound $\tilde{c}$, which in our two-dimensional computations on structured meshes takes the value $\tilde{c} = 0.2461$ for the chosen sequence of red-refined meshes.

5.3. Computation of the projection operator constant. The goal of this section is to explicitly determine the constants $C_{1,\mathrm{div}}$, $C_{2,\mathrm{div}}$, $C_{1,\mathrm{Curl}}$, $C_{2,\mathrm{Curl}}$ from (2.5) and (2.6) in the two-dimensional case. We briefly review the construction [19] and the main steps in bounding the involved constants. In order to stay close to the notation of [19] and to refer to the construction in their format, we consider the complex built by the operators ∇ and rot. By the isometry of Curl and ∇ and of rot and div in two dimensions, the results can then be used for the Curl-div complex. More precisely, after rotation of coordinates, the operator π^∇ replaces π^{Curl} from section 2.2 and the operator π^{rot} replaces π^{div} from section 2.2 (with identical stability constants).

Given a triangulation $\mathcal{T}$, we denote by $\Delta_0(\mathcal{T})$ the set of all vertices and by $\Delta_1(\mathcal{T})$ the set of all edges of $\mathcal{T}$. For any $T \in \mathcal{T}$, $\Delta_0(T)$ is the set of vertices and $\Delta_1(T)$ is the set of edges of T.

5.3.1. Falk–Winther operator for the gradient in two dimensions. Given any $y \in \Delta_0(\mathcal{T})$, the associated macroelement (or vertex patch) ω_y is defined as follows:

$$\omega_y := \operatorname{int}\left(\cup\{T \in \mathcal{T} : y \in T\}\right).$$

The subset of $\mathcal{T}$ of triangles having nonempty intersection with ω_y is denoted by $\mathcal{T}(\omega_y)$. Analogous notation applies to other open subsets $\omega \subseteq \Omega$. Given $u \in H^1(\Omega)$, the discrete function $\pi^\nabla u$ is given by its expansion

$$\pi^\nabla u = \sum_{y \in \Delta_0(\mathcal{T})} c_y(u)\lambda_y,$$

where λ_y is the piecewise linear hat function associated the vertex y, i.e., $\lambda_y(y) = 1$ and $\lambda_y = 0$ on the complement of the macroelement ω_y. The coefficient $c_y(u)$ is given by

$$c_y(u) = \fint_{\omega_y} u\,dx + (Q_y^0 u)(y),$$

where $Q_y^0 u \in S^1(\mathcal{T}(\omega_y))$ solves the discrete Neumann problem

$$\int_{\omega_y} \nabla(Q_y^0 u - u)\cdot\nabla v_h\,dx = 0 \quad \text{for all } v_h \in S^1(\mathcal{T}(\omega_y)),$$
$$\int_{\omega_y} Q_y^0 u\,dx = 0.$$

We denote by $C_1(y,T)$ the constant such that

$$|v_h(y)|^2 \leq C_1(y,T)\|\nabla v_h\|^2_{L^2(\omega_y)}$$

holds for all $v_h \in S^1(\mathcal{T}(\omega_y))$ with $\int_{\omega_y} v_h\,dx = 0$. It is readily verified that $C_1(y,T)$ is independent of the mesh size. For the actual computation of $C_1(y,T)$ we introduce bilinear forms

$$a(u,v) = u(y)v(y) \quad \text{and} \quad b(u,v) = (\nabla u, \nabla v)_{L^2(\omega_y)}$$

on the space $S^1(\mathcal{T}(\omega_y))$. It is direct to verify that $C_1(y,T)$ equals the largest eigenvalue of the generalized discrete eigenvalue problem which seeks $(\mu,u) \in \mathbb{R}\times S^1(\mathcal{T}(\omega_y))$ such that

$$a(u,v) = \mu b(u,v) \qquad \text{for all } v \in S^1(\mathcal{T}(\omega_y)). \tag{5.1}$$

Given any $T \in \mathcal{T}$, we then compute with triangle and Young inequalities

$$\|\pi^\nabla u\|^2_{L^2(T)} \leq 3 \sum_{y\in\Delta_0(T)} |c_y|^2 \|\lambda_y\|^2_{L^2(T)}.$$

For any vertex $\Delta_0(T)$ we use the definition of c_y and the definition of $C_1(y,T)$ to infer

$$\begin{aligned}|c_y|^2 &\leq 2\left(\left|\fint_{\omega_y} u dx\right|^2 + |(Q_y^0 u)(y)|^2\right)\\ &\leq 2\,\mathrm{meas}(T)^{-1}\|u\|^2_{L^2(\omega_y)} + 2C_1(y,T)\|\nabla Q_y^0 u\|^2_{L^2(\omega_y)}.\end{aligned}$$

The bound $\|\nabla Q_y^0 u\|_{L^2(\omega_y)} \leq \|\nabla u\|_{L^2(\omega_y)}$ is immediate and so concludes the stability analysis. The norm of λ_y satisfies $\|\lambda_y\|^2_{L^2(T)} = \mathrm{meas}(T)/6$. The resulting bound reads

$$\|\pi^\nabla u\|^2_{L^2(T)} \leq 3\|u\|^2_{L^2(\omega_T)} + \frac{\mathrm{meas}(T)}{h_T^2}\sum_{y\in\Delta_0(T)} C_1(y,T)\,h_T^2\|\nabla u\|^2_{L^2(\omega_T)}.$$

Summarizing, we have

$$\|\pi^{\nabla} u\|_{L^2(T)} \le C_{1,\mathrm{Curl}} \|u\|_{L^2(\omega_T)} + C_{2,\mathrm{Curl}} h_T \|\nabla u\|_{L^2(\omega_T)},$$

where

$$C_{1,\mathrm{Curl}} := \sqrt{3} \quad \text{and} \quad C_{2,\mathrm{Curl}} := \sqrt{\frac{\operatorname{meas}(T)}{h_T^2} \sum_{y \in \Delta_0(T)} C_1(y,T)}.$$

5.3.2. Falk–Winther operator for the rotation in two dimensions. The space $\mathcal{N}_0(\mathcal{T})$ is spanned by the edge-oriented basis functions $(\psi_E)_{E\in\Delta_1(\mathcal{T})}$ that are uniquely defined for any $E \in \Delta_1(\mathcal{T})$ through the property

$$\int_E \psi_E \cdot t_E \, ds = 1 \quad \text{ and } \quad \int_{E'} \psi_E \cdot t_E \, ds = 0 \quad \text{ for all } E' \in \Delta_1(\mathcal{T}) \setminus \{E\},$$

where t_E denotes the unit tangent to the edge E with a globally fixed sign. For each vertex $y \in \Delta_0(\mathcal{T})$, the piecewise constant function z_y^0 is given by

$$z_y^0 = \begin{cases} (\operatorname{meas}(\omega_y))^{-1} & \text{in } \omega_y, \\ 0 & \text{else.} \end{cases}$$

The extended edge patch of an edge $E = \operatorname{conv}\{y_1, y_2\}$ with $y_1, y_2 \in \Delta_0(\mathcal{T})$ is given by

$$\omega_E^e := \omega_{y_1} \cup w_{y_2}.$$

The piecewise constant function $(\delta z^0)_E \in L^2(\omega_E^e)$ is given by

$$(\delta z^0)_E := z_{y_1}^0 - z_{y_2}^0.$$

The Falk–Winther operator π^{rot} is defined as

$$\pi^{\mathrm{rot}} u = S^1 u + \sum_{E \in \Delta_1(\mathcal{T})} \int_E ((I - S^1) Q_E^1 u) \cdot t_E ds \, \psi_E,$$

where

$$S^1 u := M^1 u + \sum_{y \in \Delta_0(\mathcal{T})} (Q_{y,-}^1 u)(y) \nabla \lambda_y$$
$$\text{and} \quad M^1 u := \sum_{E \in \Delta_1(\mathcal{T})} \int_{\omega_E^e} u \cdot z_E^1 \, dx \psi_E.$$

The definition of the involved objects $Q_{y,-}^1$, z_E^1, Q_E^1 is as follows.

The operator $Q_{y,-}^1 : H(\mathrm{rot}, \omega_y) \to S^1(\mathcal{T}(\omega_y))$ is given by the solution of the local discrete Neumann problem

$$\begin{aligned} (u - \nabla Q_{y,-}^1 u, \nabla v)_{L^2(\omega_y)} &= 0 \qquad \text{for all } v \in S^1(\mathcal{T}(\omega_y)), \\ \int_{\omega_y} Q_{y,-}^1 u \, dx &= 0. \end{aligned}$$

We denote by $RT_{0,D}(\mathcal{T}(\omega_E^e))$ the space of elements from $RT_0(\mathcal{T}(\omega_E^e))$ with vanishing normal trace on the boundary of ω_E^e. The weight function z_E^1 is given as the solution to the following saddle-point problem: Find $(z_E^1, v) \in RT_{0,D}(\mathcal{T}(\omega_E^e)) \times S_0^1(\mathcal{T}(\omega_E^e))$ such that

$$(5.2)\qquad \begin{aligned}(\operatorname{div} z_E^1, \operatorname{div}\tau)_{L^2(\omega_E^e)} + (\tau, \operatorname{Curl} v)_{L^2(\omega_E^e)} &= (-(\delta z^0)_E, \operatorname{div}\tau)_{L^2(\omega_E^e)},\\ (z_E^1, \operatorname{Curl} w)_{L^2(\omega_E^e)} &= 0\end{aligned}$$

for all $\tau \in RT_{0,D}(\mathcal{T}(\omega_E^e))$ and all $w \in S_0^1(\mathcal{T}(\omega_E^e))$.

Given an edge E and some $u \in H(\operatorname{rot}, \omega_E^e)$, the function $Q_E^1(u) \in \mathcal{N}_0(\mathcal{T}(\omega_E^e))$ is defined by the system

$$\begin{aligned}(u - Q_E^1 u, \nabla\tau)_{L^2(\omega_E^e)} &= 0 &&\text{for all } \tau \in \mathcal{S}(\mathcal{T}(\omega_E^e)),\\ (\operatorname{rot}(u - Q_E^1 u), \operatorname{rot} v)_{L^2(\omega_E^e)} &= 0 &&\text{for all } v \in \mathcal{N}_0(\mathcal{T}(\omega_E^e)).\end{aligned}$$

We proceed by computing upper bounds to the stability constant. Let $T \in \mathcal{T}$. The triangle inequality implies

$$(5.3)\qquad \begin{aligned}\|\pi^{\operatorname{rot}} u\|_{L^2(T)} \le \|M^1 u\|_{L^2(T)} &+ \left\| \sum_{y\in\Delta_0(T)} (Q_{y,-}^1 u)(y)\nabla\lambda_y \right\|_{L^2(T)}\\ &+ \left\| \sum_{E\in\Delta_1(T)} \int_E ((I - S^1)Q_E^1 u)\cdot t_E ds\psi_E \right\|_{L^2(T)}.\end{aligned}$$

In what follows we refer to the three terms on the right-hand side as the first, second, and third terms.

Bound on the first term. Elementary estimates imply

$$\begin{aligned}\|M^1 u\|_{L^2(T)}^2 &\le \| \sum_{E\in\Delta_1(T)} |\int_{\omega_E^e} u z_E^1\,dx| |\psi_E| \|_{L^2(T)}^2\\ &\le 3\|u\|_{L^2(\omega_T)}^2 \sum_{E\in\Delta_1(T)} \|z_E^1\|_{L^2(\omega_E^e)}^2 \|\psi_E\|_{L^2(T)}^2.\end{aligned}$$

With the constant

$$C_{M_1} := \sqrt{3 \sum_{E\in\Delta_1(T)} \|z_E^1\|_{L^2(\omega_E^e)}^2 \|\psi_E\|_{L^2(T)}^2}$$

we thus have the local bound

$$\|M^1 u\|_{L^2(T)} \le C_{M_1}\|u\|_{L^2(\omega_T)}.$$

Bound on the second term. A scaling argument shows that there is a mesh-size independent constant $C_{Q,T}$ such that

$$|Q_{y,-}^1 u(y)|^2 \|\nabla\lambda_y\|_{L^2(T)}^2 \le C_{Q,T}^2 \|\nabla Q_{y,-}^1 u\|_{L^2(\omega_y)}^2.$$

The value of the constant $C_{Q,T}$ can be computed with the help of the following discrete eigenvalue problem. Define bilinear forms

$$a(u,v) = u(y)v(y)\|\nabla\lambda_y\|_{L^2(T)}^2 \quad\text{and}\quad b(u,v) = (\nabla u, \nabla v)_{L^2(\omega_y)}.$$

Then, $C^2_{Q,T}$ equals the maximal eigenvalue μ with eigenfunction $u \in S^1(\mathcal{T}(\omega_y))$ such that

$$a(u,v) = \mu b(u,v) \quad \text{for all } v \in S^1(\mathcal{T}(\omega_y)). \tag{5.4}$$

Furthermore, the stability estimate $\|\nabla Q^1_{y,-}u\|_{L^2(\omega_y)} \leq \|u\|^2_{L^2(\omega_T)}$ is immediate from the system defining $Q^1_{y,-}$. We then have

$$\begin{aligned}\left\| \sum_{y\in\Delta_0(T)} (Q^1_{y,-}u)(y)\nabla\lambda_y \right\|^2_{L^2(T)} &\leq 3 \sum_{y\in\Delta_0(T)} |(Q^1_{y,-}u)(y)|^2 \|\nabla\lambda_y\|^2_{L^2(T)}\\ &\leq 3 \sum_{y\in\Delta_0(T)} C^2_{Q,T}\|u\|^2_{L^2(\omega_y)} \leq 9C^2_{Q,T}\|u\|^2_{L^2(\omega_T)}.\end{aligned}$$

Bound on the third term. We note that there is a constant C_S such that

$$\left|\int_E (I-S^1)Q^1_E u\cdot t_E\,ds\right|^2 \|\psi_E\|^2_{L^2(T)} \leq C_S\|Q^1_E u\|^2_{L^2(\omega^e_E)}.$$

The constant C_S can be computed as the largest eigenvalue μ of the auxiliary eigenvalue

$$\int_E (I-S^1)u_h\cdot t_E\,ds \cdot \int_E (I-S^1)v_h\cdot t_E\,ds \|\psi_E\|^2_{L^2(T)} = \mu(u_h,v_h)_{L^2(\omega^e_E)} \tag{5.5}$$

on the space $\mathcal{N}_0(\mathcal{T}(\omega^e_E))$. In order to bound the norm of $Q^1_E u$, we use the discrete Helmholtz decomposition

$$Q^1_E u = \nabla\alpha_h + R,$$

where $\alpha_h \in S^1(\mathcal{T}(\omega^e_E))$ and R is a discretely divergence-free Nédélec function with homogeneous tangential boundary conditions. From a discrete Maxwell eigenvalue problem it follows that

$$\|R\|_{L^2(T)} \leq \|R\|_{L^2(\omega^e_E)} \leq c_M h_T \|\operatorname{rot} R\|_{L^2(\omega^e_E)}. \tag{5.6}$$

Moreover, from the definition of Q^1_E, we deduce the stability $\|\operatorname{rot} Q^1_E u\|_{L^2(\omega^e_E)} \leq \|\operatorname{rot} u\|_{L^2(\omega^e_E)}$. From the definition of Q^1_E, we infer from testing with $\tau = \alpha_h$

$$\|\nabla\alpha_h\|^2_{L^2(\omega^e_E)} = (u,\nabla\alpha_h)_{L^2(\omega^e_E)} \leq \|u\|_{L^2(\omega^e_E)}\|\nabla\alpha_h\|_{L^2(\omega^e_E)}.$$

This yields

$$\|\nabla\alpha\|_{L^2(\omega^e_E)} \leq \|u\|_{L^2(\omega^e_E)}.$$

The orthogonality of the decomposition therefore shows

$$\|Q^1_E u\|^2_{L^2(\omega^e_E)} = \|R\|^2_{L^2(\omega^e_E)} + \|\nabla\alpha_h\|^2_{L^2(\omega^e_E)} \leq c^2_M h^2_T \|\operatorname{rot} u\|^2_{L^2(\omega^e_E)} + \|u\|^2_{L^2(\omega^e_E)}.$$

Thus, we obtain

$$\begin{aligned}\Bigg\| \sum_{E\in\Delta_1(T)} \int_E ((I-S^1)Q_E^1 u)\cdot t_E ds \psi_E \Bigg\|_{L^2(T)}^2 &\\ \leq 3 \sum_{E\in\Delta_1(T)} \left| \int_E ((I-S^1)Q_E^1 u)\cdot t_E ds \right|^2 \|\psi_E\|_{L^2(T)}^2 &\\ \leq 9 C_S \left((c_M h_T)^2 \|\operatorname{rot} u\|_{L^2(\omega_T)}^2 + \|u\|_{L^2(\omega_T)}^2 \right). &\end{aligned}$$

We collect the bounds for the individual terms in (5.3) and conclude

$$\begin{aligned}\|\pi^{\mathrm{rot}} u\|_{L^2(T)} &\leq C_{M_1}\|u\|_{L^2(\omega_T)} + 3C_{Q,T}\|u\|_{L^2(\omega_T)} \\ &\quad + 3\sqrt{C_S}\left((c_M h_T)\|\operatorname{rot} u\|_{L^2(\omega_T)} + \|u\|_{L^2(\omega_T)}\right) \\ &\leq C_{1,\mathrm{div}}\|u\|_{L^2(\omega_T)} + C_{2,\mathrm{div}} h \|\operatorname{rot} u\|_{L^2(\omega_T)},\end{aligned}$$

where

$$C_{1,\mathrm{div}} := C_{M_1} + 3C_{Q,T} + 3\sqrt{C_S} \quad \text{and} \quad C_{2,\mathrm{div}} := 3\sqrt{C_S} c_M.$$

Remark 5.1. The discrete problems to be solved for the computation of the interpolation constants are the local discrete linear problem (5.2) and the local discrete eigenvalue problems (5.1), (5.4), (5.5) as well as the local discrete Neumann problem described in subsection 5.2 and the local discrete Maxwell eigenvalue problem related to (5.6).

5.4. Computation of the regular decomposition constant. In two dimensions the value for the constant C_{RD} from the regular decomposition equals 1. In three dimensions, assuming the domain Ω is star-shaped with respect to a ball B, estimates on the constant can be derived by tracking the constants from [24]. Sharper bounds can be expected from the solution of corresponding eigenvalue problems (similar to [20, 21]), but guaranteed inclusions require some knowledge on the distribution of the spectrum. By tracking the constants of [24] and explicit calculations we obtained the bound $C_{RD} \leq 2947$ for the unit cube in three dimensions.

6. Numerical results. In this section, we present numerical results for the two-dimensional case (and later a simple test in three dimensions). The Python implementation uses the FEniCS library [1] and the realization of the Falk–Winther operator from [25]. The two planar domains we consider are the unit square $\Omega = (0,1)^2$ and the L-shaped domain $\Omega = (-1,1)^2 \backslash ([0,1]\times[-1,0])$. The initial triangulations are displayed in Figure 2. We consider uniform mesh refinement (red-refinement). The computational bound $\hat{M}_h$ for M_h (see subsection 6.1 for actual values) is achieved with the techniques described in section 5.

6.1. Values of the individual constants. We begin by reporting our upper bounds to the individual constant entering the bound on the Falk–Winther constants. The left column of Table 1 displays the values of the constants entering the computation of the upper bound for the unit square and the L-shaped domain on structured grids with $h < \sqrt{2}/4$. All these constants coincide for the two domains, which have a similar local mesh geometry.

We compare the values with results for the unstructured mesh displayed in Figure 3. The constants for this mesh geometry are displayed in the second column of Table 1. We note that there is no significant deviation from the structured case.

FIG. 2. *Initial triangulations.*

TABLE 1
Upper bounds of some of the relevant constants for the square and the L-shaped domain (left). The same quantities for an unstructured mesh (right).

Constant	Upper bound	Constant	Upper bound
C_{M_1}	0.94974	C_{M_1}	1.31692
$C_{Q,T}$	0.66666	$C_{Q,T}$	0.66666
C_S	2.25975	C_S	2.99264
C_M	0.06522	C_M	0.06534
$C_1(y,T)$	1.05409	$C_1(y,T)$	1.05409
$\tilde{c}$	0.2461	$\tilde{c}$	0.2461
C_{OL}	13	C_{OL}	13
C_{RD}	1	C_{RD}	1
$C_{1,\text{Curl}}$	1.7321	$C_{1,\text{Curl}}$	1.7321
$C_{2,\text{Curl}}$	0.9129	$C_{2,\text{Curl}}$	0.7394
$C_{1,\text{div}}$	9.7290	$C_{1,\text{div}}$	12.29484

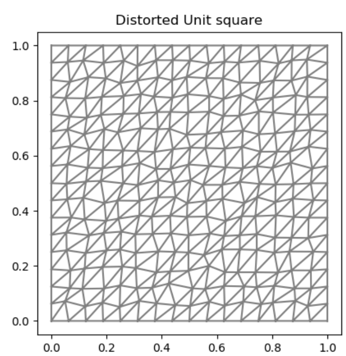

FIG. 3. *An unstructured mesh on the square domain.*

6.2. Results on the square domain. For the square domain, it is known that the first two eigenvalues are given by $\lambda_1 = \pi^2 \approx 9.8696$ and $\lambda_2 = 2\pi^2 \approx 19.7392$. The numerical results are displayed in Table 2. The displayed lower bounds are guaranteed, but their values become practically relevant after a moderate number of refinements only when M_h is sufficiently small. Higher eigenvalues are displayed in Table 3.

6.3. Results on the L-shaped domain. On the L-shaped domain, we use the reference value $\lambda = 1.4756218241$ from [16] for the first eigenvalue for comparison. The numerical results are displayed in Table 4 for eigenvalues λ_1 and λ_2 and in Table 5 for eigenvalues λ_3 and λ_4. As in the previous example, the lower bounds take values of practical significance after a couple of refinement steps.

TABLE 2
Numerical results on the square domain.

$\frac{h}{\sqrt{2}}$	κ_h	$\hat{M}_h$	$\lambda_h^{(1)}$	Lower bd.	$\lambda_h^{(2)}$	Lower bd.
2^{-1}	0.1443	9.1034	9.6000	0.0121	20.2871	0.0121
2^{-2}	0.0721	4.5499	9.8305	0.0481	20.0235	0.0482
2^{-3}	0.0356	2.2592	9.8612	0.1921	19.8205	0.1940
2^{-4}	0.0180	1.1359	9.8676	0.7186	19.7601	0.7458
2^{-5}	0.0089	0.5648	9.8691	2.3791	19.7445	2.7053
2^{-6}	0.0044	0.2806	9.8695	5.5530	19.7405	7.7269
2^{-7}	0.0023	0.1421	9.8696	8.2300	19.7395	14.1152
2^{-8}	0.0011	0.0712	9.8696	9.3992	19.7393	17.9431
2^{-9}	0.0006	0.0354	9.8696	9.7488	19.7392	19.2619

TABLE 3
Numerical results on the square domain for higher eigenvalues.

$\frac{h}{\sqrt{2}}$	$\lambda_h^{(3)}$	Lower bd.	$\lambda_h^{(4)}$	Lower bd.	$\lambda_h^{(5)}$	Lower bd.
2^{-1}	48	0.0121	57.6	0.0121	75.7128	0.0121
2^{-2}	36.8522	0.0482	46.7216	0.0483	78.5482	0.0483
2^{-3}	38.8122	0.1949	48.6686	0.1951	79.9595	0.1954
2^{-4}	39.3105	0.7600	49.1763	0.7630	79.2745	0.7675
2^{-5}	39.4362	2.9040	49.3049	2.9475	79.0401	3.0153
2^{-6}	39.4679	9.6063	49.3372	10.0980	78.9779	10.9382
2^{-7}	39.4758	21.9696	49.3453	24.7683	78.9621	30.4415
2^{-8}	39.4778	32.8925	49.3473	39.4697	78.9581	56.3816
2^{-9}	39.4782	37.6140	49.3482	46.4694	78.9572	71.8367

TABLE 4
Numerical results on the L-shaped domain.

$\frac{h}{\sqrt{2}}$	κ_h	$\hat{M}_h$	$\lambda_h^{(1)}$	Lower bd.	$\lambda_h^{(2)}$	Lower bd.
2^{-1}	0.1355	8.7947	1.3180	0.0128	3.5356	0.0129
2^{-2}	0.0709	4.5078	1.4157	0.0476	3.5309	0.0485
2^{-3}	0.0356	2.2592	1.4526	0.1726	3.5327	0.1856
2^{-4}	0.0180	1.1366	1.4667	0.5067	3.5336	0.6350
2^{-5}	0.0090	0.5682	1.4721	0.9979	3.5339	1.6506
2^{-6}	0.0045	0.2835	1.4743	1.3182	3.5340	2.7525
2^{-7}	0.0022	0.1421	1.4751	1.4324	3.5340	3.2987
2^{-8}	0.0011	0.0712	1.4754	1.4643	3.5340	3.4718

TABLE 5
Numerical results on the L-shaped domain for higher eigenvalues.

$\frac{h}{\sqrt{2}}$	$\lambda_h^{(3)}$	Lower bd.	$\lambda_h^{(4)}$	Lower bd.
2^{-1}	9.1672	0.0129	11.4797	0.0129
2^{-2}	9.6992	0.0490	11.3247	0.0490
2^{-3}	9.8272	0.1921	11.3736	0.1926
2^{-4}	9.8590	0.7177	11.3855	0.7248
2^{-5}	9.8670	2.3574	11.3885	2.4351
2^{-6}	9.8689	5.5044	11.3892	5.9472
2^{-7}	9.8694	8.2299	11.3894	9.2604
2^{-8}	9.8696	9.3992	11.3895	10.7676

TABLE 6
Numerical results on the cube domain.

$\frac{h}{\sqrt{3}}$	κ_h	$\hat{M}_h$	$\lambda_h^{(1)}$	Lower bd.
2^{-1}	0.1226	168401.5	20.7306	3.53e-11
2^{-2}	0.0992	84219.0	20.0256	1.41e-10
2^{-3}	0.0513	42110.3	19.8221	5.64e-10
2^{-4}	0.0267	21055.7	19.7600	2.26e-9

TABLE 7
Upper bounds of some of the relevant constants for the cube domain.

Constant	Upper bound
$\tilde{c}$	0.2674
C_{OL}	71
C_{RD}	2947
$C_{1,\mathrm{Curl}}$	19.7003
$C_{2,\mathrm{Curl}}$	4.5713
$C_{1,\mathrm{div}}$	57.1595

6.4. Results on the cube domain. We finally present a numerical test in three space dimensions on the cube $\Omega = (0,1)^3$. For our three-dimensional results we derive upper bounds on the Falk–Winther operator in a fashion analogous to the computations of section 5. We do not give a detailed account of these calculations because the general reasoning with the use of trace and inverse inequalities and the solution of local discrete eigenvalue problems is not different from the two-dimensional case. For the cube domain, it is known that the first eigenvalue is given by $\lambda_1 = 2\pi^2 \approx 19.7392$. The numerical results are displayed in Table 6. This table shows that our constants are too large in order to get practically relevant bounds in three dimensions. Some of the critical constants are displayed in Table 7. The results should therefore rather be seen as a proof of concept. Practically relevant bounds would require advanced computational techniques beyond our FEniCS implementation to achieve a finer spatial resolution or alternative interpolation operators with sharper stability bounds.

7. Concluding remarks. The theory on computational lower bounds to the Maxwell eigenvalues applies to the case of two or three space dimensions. The sharpness of the bounds critically depends on the actual value of $\hat{M}_h$ on coarse meshes. We remark that in two dimensions the eigenvalues coincide with the Laplace–Neumann eigenvalues, so our computations should rather be seen as a proof of concept. We succeeded in bounding M_h by $\hat{M}_h$ such that meaningful lower bounds could be achieved on moderately fine meshes. The novel ingredient is the explicit computational stability bound on the Falk–Winther operator that makes a full quantification of the Galerkin error possible. Furthermore, the methodology does not immediately generalize to adaptive meshes in the sense that κ_h is expected to scale like (some power of) the maximum mesh size. The practical use of the bounds provided by the method in three dimensions is very limited. Tighter interpolation bounds, a refined estimate of the regular decomposition constant C_{RD}, and the combination with iterative solvers will be the subject of future research.

REFERENCES

[1] M. S. Alnæs, J. Blechta, J. Hake, A. Johansson, B. Kehlet, A. Logg, C. Richardson, J. Ring, M. E. Rognes, and G. N. Wells, *The FEniCS Project Version* 1.5, Arch. Numer. Softw., 3 (2015), https://doi.org/10.11588/ans.2015.100.20553.

[2] D. N. Arnold, *Finite Element Exterior Calculus*, CBMS-NSF Regional Conf. Ser. in Appl. Math. 93, SIAM, Philadelphia, 2018, https://doi.org/10.1137/1.9781611975543.ch1.

[3] D. N. Arnold, R. S. Falk, and R. Winther, *Finite element exterior calculus, homological techniques, and applications*, Acta Numer., 15 (2006), pp. 1–155, https://doi.org/10.1017/S0962492906210018.

[4] G. R. Barrenechea, L. Boulton, and N. Boussaïd, *Finite element eigenvalue enclosures for the Maxwell operator*, SIAM J. Sci. Comput., 36 (2014), pp. A2887–A2906, https://doi.org/10.1137/140957810.

[5] G. R. Barrenechea, L. Boulton, and N. Boussaïd, *Local two-sided bounds for eigenvalues of self-adjoint operators*, Numer. Math., 135 (2017), pp. 953–986, https://doi.org/10.1007/s00211-016-0822-1.

[6] D. Boffi, *Finite element approximation of eigenvalue problems*, Acta Numer., 19 (2010), pp. 1–120.

[7] D. Boffi, F. Brezzi, and M. Fortin, *Mixed Finite Element Methods and Applications*, Springer Ser. Comput. Math. 44, Springer, Heidelberg, 2013.

[8] D. Braess, *Finite Elements. Theory, Fast Solvers, and Applications in Elasticity Theory*, 3rd ed., Cambridge University Press, Cambridge, UK, 2007.

[9] A. Buffa and I. Perugia, *Discontinuous Galerkin approximation of the Maxwell eigenproblem*, SIAM J. Numer. Anal., 44 (2006), pp. 2198–2226, https://doi.org/10.1137/050636887.

[10] E. Cancès, G. Dusson, Y. Maday, B. Stamm, and M. Vohralík, *Guaranteed and robust a posteriori bounds for Laplace eigenvalues and eigenvectors: A unified framework*, Numer. Math., 140 (2018), pp. 1033–1079, https://doi.org/10.1007/s00211-018-0984-0.

[11] C. Carstensen and J. Gedicke, *Guaranteed lower bounds for eigenvalues*, Math. Comp., 83 (2014), pp. 2605–2629.

[12] C. Carstensen and S. Puttkammer, *Direct Guaranteed Lower Eigenvalue Bounds with Optimal a Priori Convergence Rates for the bi-Laplacian*, preprint, https://arxiv.org/abs/2105.01505, 2022.

[13] T. Chaumont-Frelet, A. Ern, and M. Vohralík, *Stable broken* $\mathbf{H}(\mathbf{curl})$ *polynomial extensions and p-robust a posteriori error estimates by broken patchwise equilibration for the curl-curl problem*, Math. Comp., 91 (2021), pp. 37–74, https://doi.org/10.1090/mcom/3673.

[14] M. Costabel, *A coercive bilinear form for Maxwell's equations*, J. Math. Anal. Appl., 157 (1991), pp. 527–541, https://doi.org/10.1016/0022-247X(91)90104-8.

[15] M. Costabel and M. Dauge, *Singularities of electromagnetic fields in polyhedral domains*, Arch. Ration. Mech. Anal., 151 (2000), pp. 221–276, https://doi.org/10.1007/s002050050197.

[16] M. Costabel, M. Dauge, D. Martin, and G. Vial, *Weighted regularization of Maxwell equations: Computations in curvilinear polygons*, in Numerical Mathematics and Advanced Applications, Springer Italia, Milan, 2003, pp. 273–280.

[17] M. Costabel and A. McIntosh, *On Bogovskiĭ and regularized Poincaré integral operators for de Rham complexes on Lipschitz domains*, Math. Z., 265 (2010), pp. 297–320, https://doi.org/10.1007/s00209-009-0517-8.

[18] R. S. Falk and R. Winther, *Local bounded cochain projections*, Math. Comp., 83 (2014), pp. 2631–2656.

[19] R. S. Falk and R. Winther, *Double complexes and local cochain projections*, Numer. Methods Partial Differential Equations, 31 (2015).

[20] D. Gallistl, *Rayleigh-Ritz approximation of the inf-sup constant for the divergence*, Math. Comp., 88 (2019), pp. 73–89, https://doi.org/10.1090/mcom/3327.

[21] D. Gallistl, *A posteriori error analysis of the inf-sup constant for the divergence*, SIAM J. Numer. Anal., 59 (2021), pp. 249–264, https://doi.org/10.1137/20M1332529.

[22] D. Gallistl, P. Henning, and B. Verfürth, *Numerical homogenization of* $\mathbf{H}(\mathrm{curl})$*-problems*, SIAM J. Numer. Anal., 56 (2018), pp. 1570–1596, https://doi.org/10.1137/17M1133932.

[23] G. H. Golub, Z. Zhang, and H. Zha, *Large sparse symmetric eigenvalue problems with homogeneous linear constraints: The Lanczos process with inner-outer iterations*, Linear Algebra Appl., 309 (2000), pp. 289–306.

[24] J. Guzmán and A. J. Salgado, *Estimation of the continuity constants for Bogovskii and regularized poincare integral operators*, J. Math. Anal. Appl., 502 (2021).

[25] P. Henning and A. Persson, *Falk-Winther Projection Code Source*, Commit b9d5074, 2019, https://github.com/annaper3/falk-winther-projection.

[26] P. Henning and A. Persson, *Computational homogenization of time-harmonic Maxwell's equations*, SIAM J. Sci. Comput., 42 (2020), pp. B581–B607.

[27] R. Hiptmair, *Finite elements in computational electromagnetism*, Acta Numer., 11 (2002), pp. 237–339, https://doi.org/10.1017/S0962492902000041.

[28] F. Kikuchi and H. Saito, *Remarks on a posteriori error estimation for finite element solutions*, J. Comput. Appl. Math., 199 (2007), pp. 329–336, https://doi.org/10.1016/j.cam.2005.07.031.

[29] X. Liu, *A framework of verified eigenvalue bounds for self-adjoint differential operators*, Appl. Math. Comput., 267 (2015), pp. 341–355, https://doi.org/10.1016/j.amc.2015.03.048.

[30] X. Liu, M. T. Nakao, C. You, and S. Oishi, *Explicit a posteriori and a priori error estimation for the finite element solution of Stokes equations*, Jpn. J. Ind. Appl. Math., 38 (2021), pp. 545–559, https://doi.org/10.1007/s13160-020-00449-5.

[31] X. Liu and S. Oishi, *Verified eigenvalue evaluation for the Laplacian over polygonal domains of arbitrary shape*, SIAM J. Numer. Anal., 51 (2013), pp. 1634–1654.

[32] P. Monk, *Finite element methods for Maxwell's equations*, Oxford Science Publishing, New York, 2003.

[33] L. E. Payne and H. F. Weinberger, *An optimal Poincaré inequality for convex domains*, Arch. Ration. Mech. Anal., 5 (1960), pp. 286–292, https://doi.org/10.1007/BF00252910.

[34] K. Tanaka, A. Takayasu, X. Liu, and S. Oishi, *Verified norm estimation for the inverse of linear elliptic operators using eigenvalue evaluation*, Jpn. J. Ind. Appl. Math., 31 (2014), pp. 665–679, https://doi.org/10.1007/s13160-014-0156-2.

[35] T. Vejchodský, *Guaranteed and locally computable a posteriori error estimate*, IMA J. Numer. Anal., 26 (2006), pp. 525–540, https://doi.org/10.1093/imanum/dri043.

[36] T. Vejchodský, *Complementarity based a posteriori error estimates and their properties*, Math. Comput. Simulation, 82 (2012), pp. 2033–2046, https://doi.org/10.1016/j.matcom.2011.06.001.

[37] I. Šebestová and T. Vejchodský, *Two-sided bounds for eigenvalues of differential operators with applications to Friedrichs, Poincaré, trace, and similar constants*, SIAM J. Numer. Anal., 52 (2014), pp. 308–329, https://doi.org/10.1137/13091467X.

[38] A. Weinstein and W. Stenger, *Methods of Intermediate Problems for Eigenvalues: Theory and Ramifications,* Math. Sci. Eng. 89, Academic Press, New York, 1972.